

Stability of Al₂O₃ and Al₂O₃/*a*-SiN_x:H stacks for surface passivation of crystalline silicon

G. Dingemans,^{1,a)} P. Engelhart,² R. Seguin,² F. Einsele,³ B. Hoex,^{1,b)}
M. C. M. van de Sanden,¹ and W. M. M. Kessels^{1,c)}

¹Department of Applied Physics, Eindhoven University of Technology, P.O. Box 513, 5600 MB Eindhoven, The Netherlands

²Q-CELLS SE, Sonnenallee 17-21, 06766 Bitterfeld-Wolfen, Germany

³IEF-5, Photovoltaik, Forschungszentrum Jülich GmbH, 52425 Jülich, Germany

(Received 26 March 2009; accepted 22 October 2009; published online 4 December 2009)

The thermal and ultraviolet (UV) stability of crystalline silicon (*c*-Si) surface passivation provided by atomic layer deposited Al₂O₃ was compared with results for thermal SiO₂. For Al₂O₃ and Al₂O₃/*a*-SiN_x:H stacks on 2 Ω cm *n*-type *c*-Si, ultralow surface recombination velocities of $S_{\text{eff}} < 3$ cm/s were obtained and the passivation proved sufficiently stable ($S_{\text{eff}} < 14$ cm/s) against a high temperature “firing” process (>800 °C) used for screen printed *c*-Si solar cells. Effusion measurements revealed the loss of hydrogen and oxygen during firing through the detection of H₂ and H₂O. Al₂O₃ also demonstrated UV stability with the surface passivation improving during UV irradiation. © 2009 American Institute of Physics. [doi:10.1063/1.3264572]

Al₂O₃ synthesized by atomic layer deposition (ALD) provides a high level of surface passivation for *p*- and *n*-type crystalline silicon (*c*-Si).^{1,2} The field effect passivation associated with the negative fixed charges near the Al₂O₃/*c*-Si interface,² proved to be especially beneficial for the passivation of highly doped *p*-type *c*-Si, with Al₂O₃ even outperforming thermally grown SiO₂.³ The application of a thin Al₂O₃ film as a front passivation layer on a B-doped emitter has recently led to efficiencies as high as 23.2% for *n*-type *c*-Si solar cells.⁴ For the implementation of Al₂O₃-based passivation schemes in high-volume manufacturing of *c*-Si solar cells, the compatibility of Al₂O₃ with high temperature processing steps becomes a key issue. For example, a good thermal stability against high temperature “firing” processes of metal contacts is required for screen-printed solar cells. Research efforts on various passivation schemes have already shown that optimized *a*-SiN_x:H,⁵ *a*-SiC_x:H,⁶ SiO₂/*a*-SiN_x:H,⁷⁻⁹ SiO_x/*a*-SiN_x:H/SiO_x,¹⁰ and *a*-Si:H/*a*-SiN_x:H,¹¹ generally outperform SiO₂/SiO_x,⁹ *a*-Si:H,¹² and *a*-Si:H/SiO_x¹³ layers in terms of thermal stability. Also, the stability of the passivation scheme against ultraviolet (UV) irradiation is essential when the material is applied on an illuminated surface. In this communication, the thermal and UV stability of Al₂O₃ and Al₂O₃/*a*-SiN_x:H stacks will therefore be addressed on the basis of lifetime spectroscopy experiments. The results will be compared with those obtained for thermal SiO₂, as Al₂O₃ is a potential alternative for solar cell applications where SiO₂ would usually be considered.

The Al₂O₃ films were synthesized by remote plasma ALD by a process that consisted of alternating steps of Al(CH₃)₃ dosing and O₂ plasma oxidation. Two Oxford in-

struments reactors, the FlexAL™ and the OpAL™, were used for deposition at operating pressures of 16 and 150 mTorr and ALD cycle times of 4 and 7 s, respectively. The fact that the optimized Al₂O₃ deposition process for the FlexAL™ was readily adapted and transferred to the newly installed OpAL™ reactor without any differences in material and surface passivation properties clearly demonstrates the robustness of the ALD process. Al₂O₃ with a thickness of 30 nm, unless stated otherwise, was deposited on both sides of low resistivity (~2 Ω cm) *n*- and *p*-type double-side polished floatzone ⟨100⟩ *c*-Si wafers, which received a short dip in diluted HF (1%) prior to deposition at a temperature of ~200 °C. The Al₂O₃ passivation was activated by a post-deposition anneal at 425 °C for a 30 min time interval in N₂ environment. The thermal stability of the Al₂O₃ and Al₂O₃/*a*-SiN_x:H stacks was tested by carrying out a so-called “firing” process in an industrial beltline furnace, reaching peak temperatures >800 °C for a number of seconds. The same recipe as that for contact firing during solar cell processing was used but without the metal paste applied. The *a*-SiN_x:H, in brief SiN, was grown by remote plasma-enhanced chemical vapor deposition at temperatures of ~400 °C. The SiN films, with a thickness of ~70 nm, were optimized for antireflection coating performance. For reference, *c*-Si wafers were passivated by ~200 nm SiO₂ films grown by a wet thermal process in a tube furnace. When applied, forming gas anneals (FGAs, 10% H₂ in N₂) took place at 400 °C for 30 min. The effective lifetime of the minority carriers (τ_{eff}) was determined using a Sinton lifetime tester. The upper limit for the surface recombination velocity ($S_{\text{eff,max}}$) was calculated from τ_{eff} by assuming an infinite bulk lifetime and is quoted at an injection level of 1×10^{15} cm⁻³.

The impact of SiN deposition, postdeposition anneal, and firing on the surface passivation by Al₂O₃ is shown for a representative selection of *n*-type *c*-Si samples in Table I. Sample D coated with Al₂O₃/SiN exhibits a high lifetime

^{a)}Electronic mail: g.dingemans@tue.nl.

^{b)}Present address: Solar Energy Research Institute Singapore, National University of Singapore

^{c)}Electronic mail: w.m.m.kessels@tue.nl.

TABLE I. τ_{eff} and corresponding $S_{\text{eff,max}}$ for various $\sim 275 \mu\text{m}$ thick $2 \Omega \text{ cm}$ n -type c -Si samples passivated by Al_2O_3 or $\text{Al}_2\text{O}_3/\text{SiN}$ stacks after the successive processing steps indicated 1–3. A dash means that the process step was not carried out.

Sample	1) After annealing		2) After firing		3) After annealing	
	τ_{eff} (ms)	$S_{\text{eff,max}}$ (cm/s)	τ_{eff} (ms)	$S_{\text{eff,max}}$ (cm/s)	τ_{eff} (ms)	$S_{\text{eff,max}}$ (cm/s)
A) Al_2O_3	1.6	8.6	1.5	9.2	1.0	13.8
B) Al_2O_3	5.2	2.6	1.0	13.8	1.5	9.2
C) Al_2O_3	–	–	1×10^{-3}	1.4×10^4	1×10^{-3}	1.4×10^4
D) $\text{Al}_2\text{O}_3/\text{SiN}^a$	–	–	1.0	13.8	0.6	22.9
E) $\text{Al}_2\text{O}_3/\text{SiN}$	5.0	2.8	1.2	11.5	1.7	8.1

^aAfter deposition of the SiN capping layer, this sample revealed $\tau_{\text{eff}}=4.6 \text{ ms}$ ($S_{\text{eff,max}}=3.0 \text{ cm/s}$).

$>4 \text{ ms}$ without any postdeposition anneal. As remote plasma ALD Al_2O_3 does not provide surface passivation in the as-deposited state, reflected by lifetimes of the order of $1\text{--}10 \mu\text{s}$, it can be concluded that the thermal budget during subsequent SiN deposition was sufficient to activate the surface passivation by Al_2O_3 . Sample E was annealed after the SiN deposition, and comparable low values of $S_{\text{eff}} < 3 \text{ cm/s}$ were obtained as for sample D. Samples A and B, which were passivated by Al_2O_3 , exhibit the same level of surface passivation as the $\text{Al}_2\text{O}_3/\text{SiN}$ coated wafers. These results lead to the conclusion that the deposition of a SiN capping layer does not compromise the quality of the Al_2O_3 surface passivation, which is in agreement with the excellent performance of solar cells incorporating $\text{Al}_2\text{O}_3/\text{SiN}$ stacks.⁴

Subsequently, the samples were exposed to the high temperature firing step. The effective lifetime of sample B (Al_2O_3) and samples D and E ($\text{Al}_2\text{O}_3/\text{SiN}$) decreased during firing, but remained in the millisecond range. The lifetime of sample A remained constant during firing, which could indicate that, for this sample, bulk recombination instead of surface recombination largely determines the effective lifetime. From these observations, we infer that a SiN capping layer does not increase the already good thermal stability of the Al_2O_3 passivation scheme, which contrasts with observations for a -Si:H and SiO_2 passivation schemes.^{5,7–11} Values of $S_{\text{eff,max}} < 14 \text{ cm/s}$ after firing Al_2O_3 suggest that surface recombination will not be the efficiency limiting step for solar cells that combine Al_2O_3 passivation and screen printed metallization as recombination in the metalized area will dominate.¹⁴ The firing stability of Al_2O_3 with a metal layer atop however still needs to be investigated.

Sample C, without postdeposition anneal and with a lifetime in the μs -range, demonstrates that the firing process does not activate the Al_2O_3 surface passivation. Also, a subsequent anneal did *not* improve the measured lifetime. Annealing after the firing process resulted in a slight decrease of lifetime for samples A and D, whereas some improvement of the surface passivation was observed for samples B and E. Also, a FGA could not significantly improve the level of surface passivation after firing. The observations, as listed in Table I, clearly indicate that the relatively minor decrease in surface passivation by Al_2O_3 during firing cannot be restored by an additional anneal.

To benchmark the *thermal stability* of Al_2O_3 , c -Si wafers were passivated by SiO_2 with subsequent FGA. Figure 1

shows injection level dependent τ_{eff} for SiO_2 and Al_2O_3 samples measured before and after firing, and for SiO_2 also after a successive FGA after firing. The exceptionally high effective lifetime for the SiO_2 passivated sample (with $\tau_{\text{eff}}=3.7 \text{ ms}$ and $S_{\text{eff}} < 3.5 \text{ cm/s}$) decreases due to the firing process to values of $\sim 5 \mu\text{s}$, indicating that the surface passivation is completely lost, in agreement with observations by Schultz *et al.*⁹ A subsequent FGA can reactivate the surface passivation by SiO_2 after firing to some extent ($S_{\text{eff}} < 115 \text{ cm/s}$). The passivation by SiO_2 , which is predominantly chemical in nature (passivation of surface defects), can be improved by hydrogenation during annealing.¹⁵ The passivation by Al_2O_3 , which is a combination of chemical passivation with a strong field-effect passivation,² clearly shows a much higher stability against firing. However, the minor decrease in surface passivation could not be improved by hydrogenation during FGA (not shown here). Moreover, the hydrogen released from the SiN capping layer during firing^{10,15} did also not lead to such an improvement, as concluded from Table I.

Apparently, the Al_2O_3 surface passivation is affected differently by the firing process than thermal SiO_2 . Therefore, to gain more insight into the influence of the firing process on the Al_2O_3 properties, effusion experiments were carried out. In an ultrahigh vacuum quartz tube with a base pressure $< 10^{-7} \text{ mbar}$, a c -Si wafer double-side coated with 100 nm Al_2O_3 was heated up to $1000 \text{ }^\circ\text{C}$ with a constant heating rate of $20 \text{ }^\circ\text{C}/\text{min}$.¹⁶ A quadrupole mass spectrometer detected the hydrogen and other volatile species that desorbed from

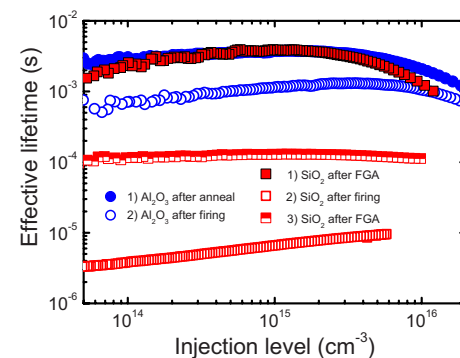


FIG. 1. (Color online) Effective lifetime vs injection level for $2 \Omega \text{ cm}$ n -type c -Si passivated by Al_2O_3 and $2 \Omega \text{ cm}$ p -type c -Si passivated by SiO_2 , after successive processing steps indicated 1–3.

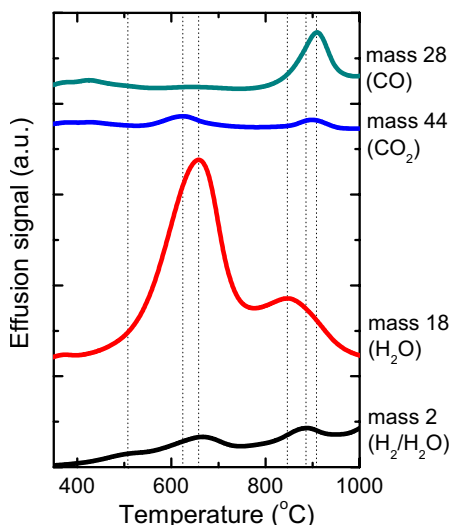


FIG. 2. (Color online) Thermal effusion transients at mass-over-charge ratios 2, 18, 28, and 44 for *c*-Si double-side deposited with 100 nm Al_2O_3 . From mass spectrometry cracking patterns, the most likely parent molecules contributing to the signals at the selected mass-to-charge ratios have been determined. The transients are offset for clarity.

the sample at elevated temperatures. In Fig. 2, we show the effusion of H_2 , H_2O , CO , and CO_2 at high temperature as these were the majority species released from the Al_2O_3 sample. Distinct effusion peaks are observed at 625 °C for CO_2 and at 910 °C for CO_2 and CO . The formation of these volatile species indicates the incorporation of CO_x impurities into the Al_2O_3 bulk by remote plasma ALD.¹⁷ Effusion peaks also appear in the transients at 660 °C for H_2O and H_2 (with the H_2 signal probably mainly originating from H_2O), at 850 °C for H_2O , and at 890 °C for H_2 . In addition, a small H_2 feature is observed in the spectrum at 510 °C, which could possibly originate from cracking C_xH_y species that were detected through mass 15 and 29. The detection of H_2O and H_2 is consistent with the presence of a significant density of $-\text{OH}$ groups in the Al_2O_3 bulk as confirmed by infrared spectroscopy, Rutherford backscattering spectroscopy, and elastic recoil detection analysis revealing slightly O-rich films (O/Al ratio = ~ 1.5 – 1.6) with a hydrogen concentration of ~ 3 at. % in the as-deposited Al_2O_3 . From Fig. 2, we conclude that the effusion from the Al_2O_3 films at temperatures up to 800 °C is dominated by the formation and release of H_2O . Apparently, hydrogen in the form of H_2 is primarily released from the film at temperature >800 °C. Consequently, during a firing process, the Al_2O_3 loses both hydrogen and oxygen which indicates significant structural changes of the Al_2O_3 film that adversely affect the passivation. Furthermore, hydrogen is depleted from the film predominantly in the form of H_2O which is different from the dehydrogenation of SiO_2 /*c*-Si interface after firing. The depletion of hydrogen from the Al_2O_3 /*c*-Si interface likely contributes to the decrease of the surface passivation by Al_2O_3 after firing.^{2,18,19} Furthermore, the structural changes of the Al_2O_3 will render the influence of the firing step irreversible.

Apart from thermal stability, long term and UV stability are also important criteria for *c*-Si surface passivation. The

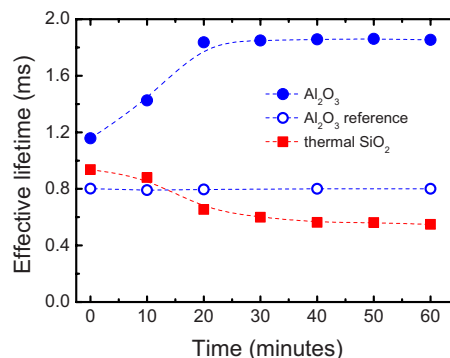


FIG. 3. (Color online) Effective lifetime vs UV exposure time for Al_2O_3 and SiO_2 passivated 2 Ω cm *p*-type *c*-Si samples. The reference sample was not exposed to UV and kept under indoor light conditions during the time indicated. Lines serve as guides to the eye.

long term stability of the passivation by Al_2O_3 was verified by monitoring a large number of passivated *c*-Si wafers over time up to six months. No degradation of the measured effective lifetime was observed. In fact, a significant number of samples exhibited even a *positive aging* effect after anneal, an effect of which the physical origin is still subject of research. The stability of the Al_2O_3 passivation against UV photons was tested by exposing various lifetime samples to UV irradiation during time intervals of 10 min alternating between the sample surfaces exposed. A ~ 100 W Hg lamp was used as UV source, which emits predominantly at 254 nm (4.9 eV). The distance between lamp and sample was kept at ~ 10 cm to avoid significant sample heating. It was verified that the surface passivation of an as-deposited sample could not be activated by UV irradiation for the conditions employed. For comparison, the experiment was also carried out for SiO_2 passivated sample (from a different wafer ingot than the sample in Fig. 1), which received a so-called *aneal*²⁰ at 425 °C for 15 min to activate the passivation. Figure 3 shows τ_{eff} as a function of cumulative exposure time for representative samples. The effective lifetime of the Al_2O_3 coated sample increased up to 40% after exposing both wafer surfaces. Additional UV irradiation did not result in a significant further increase of τ_{eff} . The lifetime of the SiO_2 passivated sample, on the other hand, was observed to decrease under UV irradiation, which can be attributed to a higher interfacial defect density created by the incoming photons.^{20,21} Both the improved surface passivation by Al_2O_3 and the degraded passivation by SiO_2 remained stable over time. We explain the improvement of the Al_2O_3 surface passivation under UV exposure by a significant increase of the fixed negative charge density, which was already reported in the pioneering work of Hezel *et al.* for pyrolysis-grown Al_2O_3 .²² This photon induced charge injection process was recently also observed for Al_2O_3 films synthesized by ALD during a laser spectroscopic study.²³ A similar beneficial effect from charge injection was also reported for AlF_3 films.²⁴ Furthermore, the reported UV stability of the interface defect density²² suggests that the impact of UV irradiation on the *chemical* passivation by Al_2O_3 is less significant.

In summary, the surface passivation provided by atomic layer synthesized Al_2O_3 was found sufficiently stable under a

high temperature firing step, with the surface recombination velocities remaining as low as <14 cm/s after reaching temperatures >800 °C. Effusion measurements revealed the loss of hydrogen and oxygen from the Al_2O_3 during firing through the detection of H_2 and H_2O indicating structural changes within the material. The application of a SiN capping layer affected neither the level of surface passivation nor the thermal stability of the Al_2O_3 significantly. The thermal stability that was demonstrated, in conjunction with the long term and UV stability, are prerequisites for the application of Al_2O_3 passivation schemes in high-volume manufactured solar cells.

W. Keuning (TU/e), Dr. W. Beyer (IEF-5 Jülich), K. Regenbrecht, and Dr. S. Wanka (Q-CELLS) are acknowledged for technical support and/or discussions.

- ¹B. Hoex, J. Schmidt, P. Pohl, M. C. M. van de Sanden, and W. M. M. Kessels, *J. Appl. Phys.* **104**, 044903 (2008).
²B. Hoex, J. J. H. Gielis, M. C. M. van de Sanden, and W. M. M. Kessels, *J. Appl. Phys.* **104**, 113703 (2008).
³B. Hoex, J. Schmidt, R. Bock, P. P. Altermatt, M. C. M. van de Sanden, and W. M. M. Kessels, *Appl. Phys. Lett.* **91**, 112107 (2007).
⁴J. Benick, B. Hoex, M. C. M. van de Sanden, W. M. M. Kessels, O. Schultz, and S. W. Glunz, *Appl. Phys. Lett.* **92**, 253504 (2008).
⁵B. Lenkeit, S. Steckemetz, F. Artuso, and R. Hezel, *Sol. Energy Mater. Sol. Cells* **65**, 317 (2001).
⁶I. Martin, M. Vetter, A. Orpella, J. Puigdollers, C. Voz, L. F. Marsal, J. Pallares, and R. Alcubilla, *Thin Solid Films* **403-404**, 476 (2002).
⁷J. Schmidt, M. Kerr, and A. Cuevas, *Semicond. Sci. Technol.* **16**, 164 (2001).

- ⁸V. D. Mihaletchi, Y. Komatsu, and L. J. Geerlings, *Appl. Phys. Lett.* **92**, 063510 (2008).
⁹O. Schultz, M. Hofmann, S. W. Glunz, and G. P. Willeke, Proceedings of the 32nd IEEE Photovoltaic Specialists Conference, Lake Buena Vista, FL, 3–7 January 2005 (IEEE, New York, 2005), p. 872.
¹⁰M. Hofmann, S. Kambor, C. Schmidt, D. Grambole, J. Rentsch, S. W. Glunz, and R. Preu, *Adv. OptoElectron.* **2008**, 485467 (2008).
¹¹S. Gatz, H. Plagwitz, P. P. Altermatt, B. Terheiden, and R. Brendel, *Appl. Phys. Lett.* **93**, 173502 (2008).
¹²S. Dauwe, J. Schmidt, and R. Hezel, Proceedings of the 29th IEEE Photovoltaic Specialists Conference, New Orleans, LA, 20–24 May 2002 (IEEE, New York, 2002), p. 1246.
¹³M. Hofmann, C. Schmidt, N. Kohn, J. Rentsch, S. W. Glunz, and R. Preu, *Prog. Photovoltaics* **16**, 509 (2008).
¹⁴J. Schmidt, A. Merkle, R. Brendel, B. Hoex, M. C. M. van de Sanden, and W. M. M. Kessels, *Prog. Photovoltaics* **16**, 461 (2008).
¹⁵M. McCann, K. Weber, and A. Blakers, *Prog. Photovoltaics* **13**, 195 (2005).
¹⁶W. Beyer, J. Herion, H. Wagner, and U. Zastrow, *Philos. Mag. B* **63**, 269 (1991).
¹⁷E. Langereis, J. Keijmel, M. C. M. van de Sanden, and W. M. M. Kessels, *Appl. Phys. Lett.* **92**, 231904 (2008).
¹⁸S. Jakschik, U. Schroeder, T. Hecht, D. Krueger, G. Dollinger, A. Bergmaier, C. Luhmann, and J. W. Bartha, *Appl. Surf. Sci.* **211**, 352 (2003).
¹⁹S. Zafar, A. Callegari, V. Narayanan, and S. Guha, *Appl. Phys. Lett.* **81**, 2608 (2002).
²⁰W. Füssel, M. Schmidt, H. Angermann, G. Mende, and H. Flietner, *Nucl. Instrum. Methods Phys. Res. A* **377**, 177 (1996).
²¹P. E. Gruenbaum, R. R. King, and R. M. Swanson, *J. Appl. Phys.* **66**, 6110 (1989).
²²R. Hezel and K. Jaeger, *J. Electrochem. Soc.* **136**, 518 (1989).
²³J. J. H. Gielis, B. Hoex, M. C. M. van de Sanden, and W. M. M. Kessels, *J. Appl. Phys.* **104**, 073701 (2008).
²⁴D. Konig, D. R. T. Zahn, and G. Ebest, *Appl. Surf. Sci.* **234**, 222 (2004).